PHYSICAL REVIEW E **83**, 051606 (2011)

# Lipid aggregate formation at an oscillating bubble surface: A simulation study

Joost H. J. van Opheusden and Jaap Molenaar
*Biometris, Department of Mathematical and Statistical Methods, Wageningen University, Droevendaalsesteeg 1, NL-6708 PB Wageningen, The Netherlands*

(Received 16 July 2010; revised manuscript received 17 February 2011; published 19 May 2011)

We perform a molecular dynamics simulation study of the behavior of a lipid coating layer on an oscillating bubble surface. Micrometer sized bubbles, stabilized with a lipid monolayer coating, are used in acoustic imaging as a contrast agent. The coating layer is expected to be strongly influenced by the oscillation of the bubble in the high frequency sound field, with a period of a microsecond. The typical time scale of molecular motion, however, is of the order of femtoseconds. One of the challenges is to bridge this nine decade gap in time scales. To this end we have developed a model that is highly coarse grained, but still features the essential mechanisms determining lipid dynamics, with time scales of picoseconds. This approach allows us to severely restrict the computing times, although we make use of very modest computing equipment. We show in our simulation that the amphiphilic monolayer folds upon contraction of the bubble, and forms micellar aggregates at the air-water interface. Some micellar structures survive consecutive re-expansion and indeed remain persistent over several cycles. These structures may add to the anisotropic behavior of the bubbles under oscillating conditions. We also investigated temperature and frequency dependence.

DOI: 10.1103/PhysRevE.83.051606 PACS number(s): 68.03.Hj, 02.70.−c, 62.20.mq, 62.25.De

## I. INTRODUCTION

Micrometer sized air bubbles are used in acoustic imaging as a contrast agent [1]. When these bubbles are injected into the bloodstream and exposed to a high frequency sound field, of the order of a few MHz, their resonance enhances the reflected signal. To stabilize the bubbles they are coated with lipids that form a monolayer on the air-water interface. The amplitude of the oscillations is large; the total surface area of the bubble changes by 30% and more, as has been observed directly in high speed optical imaging of oscillating bubbles under a microscope [2,3]. The lipid monolayer on these bubbles is strongly influenced by the oscillations of the bubble. Upon compression the monolayer goes from a vaporlike state in which polydisperse compact patches of lipids coexist with individual lipids to a compact liquidlike state. When compressed further, the monolayer is thought to form folds, and buckle [4,5]. The high speed images of individual coated bubbles in an acoustic field have also shown that their deformation is often quite anisotropic and nonlinear [6,7]. The nonlinear response leads to lower harmonics in the reflected sound, which are specifically interesting for applications, since they provide an opportunity to use filtering techniques for image enhancement. While hydrodynamic effects can be responsible for nonspherical behavior, the observed anisotropy is persistent over several oscillations, suggesting the development of structure in the bubble, presumably in the coating layer. To investigate the latter supposition, we perform a simulation study of the effect of the oscillations in bubble size on the coating layer and expect to find the forming of micelles. Here we use the term micelle to describe any long-lived association of lipids other than a monolayer at the air-water surface. Since these micelles will come into existence at random positions, this could explain the observed anisotropy.

In the literature, a few models have been published that describe the effect of a coating on the oscillations of a bubble in a periodic pressure field [8]. Marmottant [9] uses a simple empirical relation for the surface tension of a coated bubble as a function of its radius. Numerical solution of the Rayleigh-Plesset equation then reproduces many of the features mentioned above. The model does assume that the compression and expansion of the monolayer is reversible and that the period of the periodic forcing is large enough to have no hysteresis effects. The nonlinearities are quite well captured by this theory, but the anisotropy is not included. Also the folding and buckling of the layer is not directly included.

The formation of folds and possibly supramolecular structures like micelles, involves processes at the molecular scale, at time scales that are significantly lower than the bubble oscillation period. The high frequency acoustic waves, with a period of the order of a microsecond, which are responsible for the oscillation of the bubbles, are in fact quite slow on a molecular time scale of femtoseconds. That implies that not all molecular details may be relevant for the response of the layer to the oscillations. To bridge the nine decades in time scale we use a very coarse grained model, which ignores most of the internal motions of the lipids, such as rotational bond vibrations, and the water. Monodisperse Lennard-Jones particles are used to simulate the water, while the lipids are modeled as dumbbells. A single water phase particle stands for a large number of actual water molecules. All molecular detail of the water and the lipids, including the electromagnetic dipole, is fully neglected. The air phase is treated as a vacuum.

In a very large scale dynamical simulation of such a monolayer [10], using a much more detailed model than in the present study, a similar system was shown to be able to produce a single micelle (a double layer vesicle) at an air-water surface under compression. A consecutive re-expansion was not studied. Vesicle formation was found earlier in experiments [11,12]. Our simplified model allows us to follow the system on the relevant time scales with standard molecular dynamics techniques for several oscillation periods, on very modest computing equipment, at oscillation frequencies from 2 to 200 MHz. We show that within our model the monolayer folds upon contraction beyond dense packing, in which process individual lipids or small patches of lipids are moved inward,

 

toward the air phase. These consequently form lipid aggregates at the air-water interface that we call micelles. They are in fact small patches of a double layer or multilayer, somewhat similar to inverted micelles in oil. At the high frequencies these structures are irreversibly formed; they only partly disappear upon expansion. Also there is a hysteresis loop associated with the ordering of the monolayer; it reacts differently upon expansion and compression. The formation of these structures adds to the nonlinearity of the system. At low frequencies our model system reacts more reversible and linear.

## II. SIMULATION MODEL

We investigate the dynamics of a lipid monolayer on a periodically compressed and expanded air-water interface with standard molecular dynamics (MD); the system consists of point mass particles that interact through pair potentials, and their dynamics is described by Newtonian equations of motion.

### A. Representation of the sample

The water phase is represented by monodisperse spherical particles with a 6-12 Lennard-Jones (LJ) interaction, cut off at a distance of $r = 2.5\sigma$,

$$V_{\mathrm{LJ}}(r) = 4\varepsilon\left[\left(\frac{\sigma}{r}\right)^{6} - \left(\frac{\sigma}{r}\right)^{12}\right], \quad r \leqslant 2.5\sigma. \tag{1}$$

This implies that for large distances ($r > 2.5\sigma$) the particles have no interaction, for intermediate distances ($\sigma < r < 2.5\sigma$) they have a van der Waals type attraction, and at short distances ($r < \sigma$) there is a strong repulsion.

The lipids are represented as LJ dumbbells, where the head groups have the same characteristics as the water phase particles. The other part of the dumbbell represents the hydrophobic tails. These particles mutually have the same LJ interaction as the water phase particles. For the interaction between water type and tail type we use a Weeks-Chandler-Andersen (WCA) potential, which is just the repulsive part of the LJ interaction, implemented by using a cutoff of $r = 1.12\sigma$. The two parts of the dumbbell are connected through a Hookean spring potential with rest length $\sigma$,

$$V_H(r) = \tfrac{1}{2}k(r-\sigma)^2. \tag{2}$$

The system is placed in a periodic three-dimensional (3D)-image box, which is elongated in the vertical direction. In the center of the box a horizontal slab of water-type particles is placed, coated on both sides with a monolayer of lipidlike dumbbells, as shown in Fig. 1. This allows us to maintain periodicity, without introducing an air-water interface.

### B. Time integration

The motion of the $N$ particles is integrated numerically with a time step $\Delta t$ using a leapfrog method for their positions $x_i(t)$ and velocities $v_i(t)$,

$$\begin{cases} v_i\left(t+\frac{1}{2}\Delta t\right) = v_i\left(t-\frac{1}{2}\Delta t\right) + \Delta t a_i(t) \\ x_i\left(t+\Delta t\right) = x_i(t) + \Delta t v_i\left(t+\frac{1}{2}\Delta t\right) \\ a_i(t) = -\dfrac{1}{m}\nabla_x V[x_i(t)] = \dfrac{1}{m}F_i(t), \quad i = 1\ldots N \end{cases} \tag{3}$$

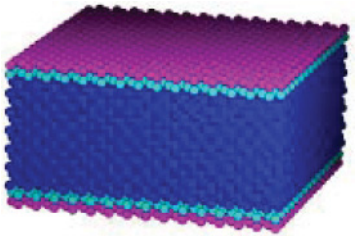

FIG. 1. (Color online) Initial configuration of the sample; just a single periodical box is shown. Two coating layers are separated by a water layer. Waterlike particles are colored blue (dark gray), hydrophilic lipid head groups are cyan (light gray), and hydrophobic tail groups are magenta (medium gray). Depth cueing is implemented by diminishing the brightness of the particle color with distance. The two coating layers are separated by a sufficiently thick water layer to be considered independent.

with $V$ the sum of all interactions with other particles.

During the simulated motion, rounding errors and compression and expansion of the box can cause the average particle velocity, and hence the temperature, to change. Thermostatting is implemented by a rescaling of the individual particle velocities after each time step to keep the average (rms) velocity close to the one set by the required temperature:

$$\tfrac{1}{2}m\langle v^2\rangle = \tfrac{3}{2}k_B T \tag{4}$$

The rescaling factor we apply to all velocities is

$$v_{\mathrm{scaled}} = \frac{1}{2}v_{\mathrm{num}}\left(1 + \sqrt{\frac{3k_B T}{m\langle v_{\mathrm{num}}^2\rangle}}\right), \tag{5}$$

where $v_{\mathrm{num}}$ is the velocity according to the numeric leapfrog algorithm. By rescaling only partially we avoid large fluctuations due to numerical instability, similar to what is done in conjugate gradient methods. The actual temperature hence is allowed to show some fluctuation. In practice during the quasiequilibrium runs, the temperature hardly varies.

### C. Compression and expansion

Compression and expansion of the bubble is emulated by small changes in the horizontal size of the image box at each integration step. During such changes also the positions of all particles are changed affinely to give a uniform homogeneous change. Local fluctuations in the structure and composition of the model system make it relax inhomogeneously to such disturbances. During lateral expansion the water layer will become thinner in the vertical direction and under compression it will become thicker. The box is taken sufficiently elongated in the vertical direction to avoid the two sides coming into contact upon compression. Particles escaping from the layer may travel along the vertical direction. If they leave the box via the lower or upper box wall, they come back via the other side thanks to the periodicity of the box.

### D. Scaling of variables

For numerical convenience the mass $m$ of the particles, the depth $\varepsilon$ of the LJ minimum, and the LJ length scale $\sigma$ are all normalized to unity in the calculations. That implies that the

time scale of the fluctuations around the LJ minimum is also unity,

$$\tau_{\mathrm{LJ}} = \sqrt{\frac{m\sigma^2}{\varepsilon}} = 1. \tag{6}$$

The fluctuations about the equilibrium bond length are typically (much) faster,

$$\tau_k = \sqrt{\frac{m}{k}} = \sqrt{\frac{1}{k}}. \tag{7}$$

A value of $k = 100$ was used throughout all runs, so $\tau_k = 0.1$. To reduce numerical inaccuracy a time step of $\Delta t = 0.02$ was used in all runs, sufficiently small compared to $\tau_k$ for the leapfrog algorithm to accurately integrate the motions.

The actual time scale can be related to thermal motions in the system. The time it takes a particle to move across a distance of the order of its own size due to thermal motion is

$$\tau_{\mathrm{kin}} = \frac{\sigma}{v_{\mathrm{rms}}} = \sqrt{\frac{m\sigma^2}{k_{\mathrm{B}}T}}. \tag{8}$$

For real lipids, typical figures are $m = 10^{-24}$ kg, and $\sigma = 10^{-9}$ m, while $k_{\mathrm{B}} = 1.38 \times 10^{-23}$ J/K, and room temperature $T = 300$ K, so $\tau_{\mathrm{kin}} = 1.5 \times 10^{-11}$ s. In our simulation runs we used a temperature of $k_{\mathrm{B}}T = 0.5$, which corresponds to $\tau_{\mathrm{kin}} = 1.5$. In other words, a time unit in the simulation corresponds to 10 ps in the real system. This is substantially larger than the femtosecond time scales in ordinary molecular simulation. With a time step of $\Delta t = 0.2$ ps and a box oscillation frequency of 5 MHz, a single period run lasts 200 ns, which amounts to 1 000 000 iteration steps.

### E. Order parameter

To follow the development of structure in the lipid coating layers, we introduce an order parameter measuring the orientation of the dumbbells. For each dumbbell we take the cosine of the angle with respect to the vertical direction, the positive direction for the upper and the negative direction for the lower layer. The order parameter is the average over all dumbbells:

$$\lambda = \frac{1}{N_{\mathrm{lipids}}} \sum_{\mathrm{lipids}} \cos(\theta_i). \tag{9}$$

A value of $\lambda = 1$ corresponds to perfect order in the lipid layer, with all lipids standing in parallel, upright positions; lower values of $\lambda$ indicate less ordered states.

### F. Equipment

The simulation results presented here were all obtained on a simple standard PC with a 1.8 GHz AMD® Athlon dual core processor, using private FORTRAN code. For the sample size as used, each time step takes about 0.25 s calculation time on this PC (using a single core), a single period run at 5 MHz box oscillation frequency takes about 70 h.

## III. RESULTS

### A. Initial setup and relaxation

We first discuss the results of calculations performed for the equilibration of a slab at a low lateral lipid density. In the initial state the water particles are placed on a regular fcc lattice (Fig. 1). The lipid dimers are added with their hydrophilic head groups on an fcc lattice site (two for each box) and the hydrophobic tail pointing straight up or down, respectively, for the upper and lower interface layer. In this configuration the order parameter is exactly unity. Note that we have two independent monolayers. The slab configuration avoids separate boundary conditions for the water phase. We used a system of 15 fcc unit boxes in the horizontal directions, with a periodic image box size of 30 (in units scaled to $\sigma$), and six unit boxes in the vertical direction, with an image box size of 120. As each fcc unit box contains four particles, the total number of waterlike particles is 5400. Each layer of lipids consists of 450 dimers. The two layers are separated by a water layer that is thick enough to consider the two layers at the top and the bottom as being independent.

With an fcc-box size of 2 the nearest neighbor distance is 1.4. Since the LJ minimum is at 1.2, the sample may be expected to shrink substantially. Because of the periodic boundary conditions, it can only do so in the vertical direction. The initial regularity is broken rapidly, because the initial velocities are chosen randomly from a Maxwell-Boltzmann distribution at the chosen temperature of $k_{\mathrm{B}}T = 0.5$. The approach to equilibrium is monitored by inspection of the overall total energy. In 50 time units, 0.5 ns real time, the system relaxes. Then, it reaches a disordered liquidlike structure and the initial crystalline order is rapidly destroyed.

The image in Fig. 2 shows the sample at the end of the equilibration run. As can be observed, the slab is much less thick, and the regular order has fully disappeared. The surface layer is not really flat, and when seen from directly above, the lipid coverage of the water surface is observed to be patchy;

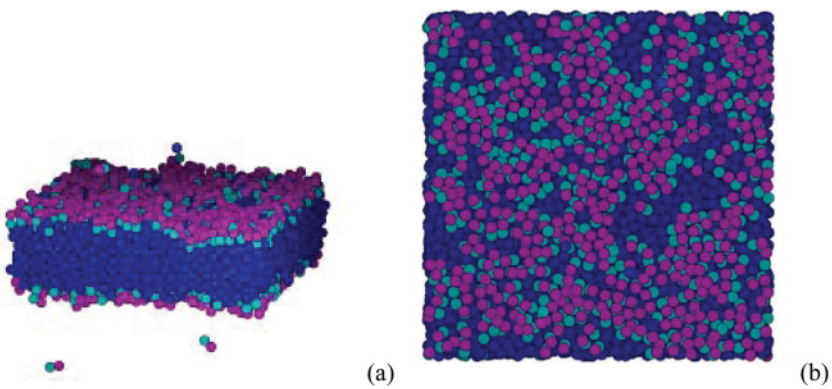


FIG. 2. (Color online) Snapshot of the sample after 0.5 ns relaxation. In the vertical direction the sample is condensed considerably (a). The coating layer, as seen from above (b), has become rather patchy, leaving parts of the water surface exposed.

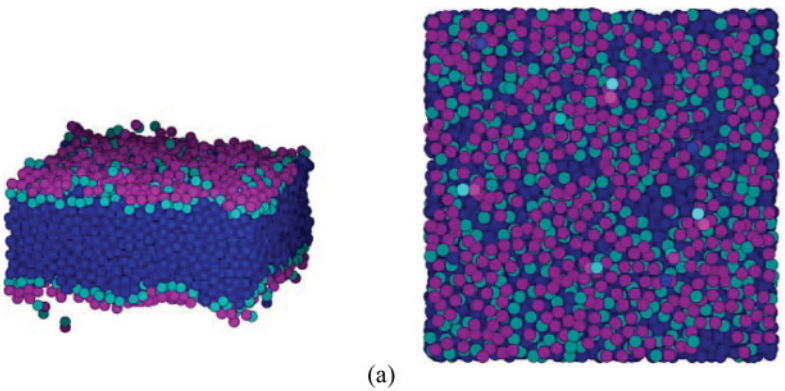


FIG. 3. (Color online) Side (a) and top (b) view of the sample after compression to a lateral lipid density where they almost fully cover the surface. The lateral order is still far from regular (b), and a few lipids have moved out of the monolayer (a); some have even "evaporated" by escaping the layer as a whole

the monolayer is in a dilute state, some parts of the water surface are not covered, but are exposed to the air. The lipids form small clusters, within which the lateral ordering is rather random. At the edges of the clusters the lipids tend to lie flat on the surface. Between the clusters, there are holes in the layer, which are void of lipids, where the water surface is in direct contact with the air. The order parameter drops to a value of about 0.75.

### B. Compression and expansion

When the initially dilute system is subjected to a compression-expansion cycle, more condensed states of the monolayer are obtained. We consider a cycle of 500 time units, a 5-ns period, or 200 MHz, where the lateral box sizes undergoes a sinusoidal change between the initial 30 and 20 length units. Figure 3 contains a snapshot of the system in a more dense state, with a lateral box size of 26.5. At this lateral lipid density a perfectly regular fcc lattice covering the surface would be the energetically favored state, but entropically it is not. In practice the lipids still almost fully cover the water surface, but the order in the monolayer(s) remains more or less constant during the compression, instead of increasing, as it would if crystallization would occur. A few lipids have moved out of the monolayer, but still remain attached to the surface, as can be seen in Fig. 3(a), These particles have their (light colored) head group exposed to the air. Some lipids have fully escaped the slab.

Further compression of the sample leads to more lipids moving out of the monolayer and forming an inverted layer on top of it. In the most compressed state we have used in this study, at lateral box size of 20, the lipids are literally squeezed out (Fig. 4). The lipids with the head groups pointed to the air phase are clearly visible. The layer as a whole also folds, as can be seen in Fig. 4(a), which shows the sample from the side. The lower layer in this image is seen to react similarly. Due to the lateral compression, the water phase has extended in the vertical direction; the slab is much thicker than in the starting configuration at box size 30.

When the compressed sample is expanded back to the original box size, most of the lipids move back to the monolayer, but some stay in the double layer configuration (see Fig. 5). The structure that has formed upon compression does not disappear completely upon expansion. The order parameter returns to a maximal value of 0.65, also indicating that part of the micellarlike structures that were formed do not fall apart in the time scale of the current cycle.

### C. Order parameter dynamics

We have followed the order parameter in the sample for five consecutive periods. After the initial drop the cycle more or less repeats itself (Fig. 6). The fluctuations for the small sample are quite large. At the initial compression of the diluted sample the order parameter stays roughly constant. In the first 100 time units the gaps in the monolayer where the water is exposed to the air are closed, but the lipid patches remain largely unaltered. After that the order parameter drops rapidly to a value of about 0.35. In fact, the order parameter continues dropping when the box is already expanding, indicating that

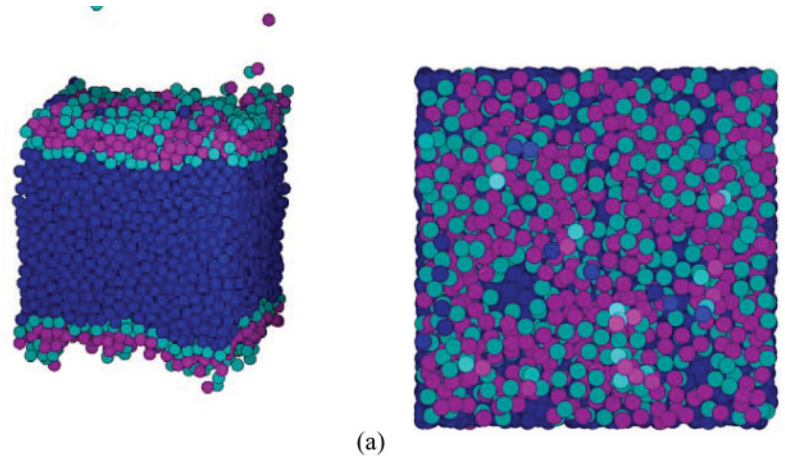


FIG. 4. (Color online) Compressed sample. The lateral box size has been decreased from 30 to 20, giving more than a factor of 2 reduction in surface area. The side view (a) shows bending of the layer, the top view (b) shows several patches of double layer.

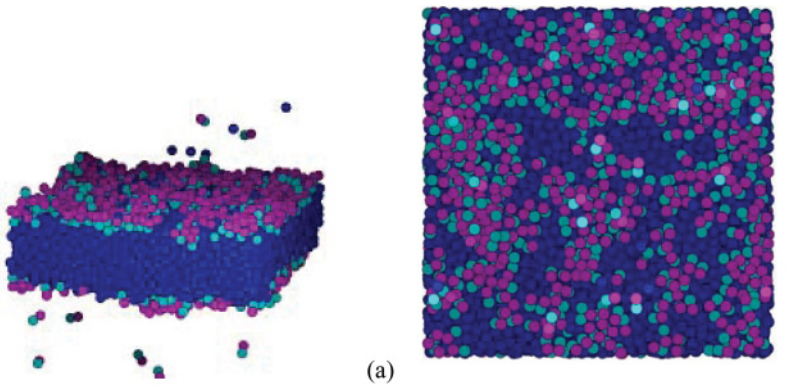


FIG. 5. (Color online) Re-expanded sample. When the lateral box size is brought back to the 30 units, the lipid coverage of the surface breaks up into patches again, but some bilayer structure remains. Compared to Fig. 2(b) the exposed part of the water surface is considerably larger.

more double layer structures are being formed spontaneously. The following increase in order during further expansion is more gradual, and again the maximum is reached when the sample is already being compressed again. Not only is there a distinct phase difference between the driving force (sample size) and the effect (order parameter), but the behavior of the latter also shows distinct nonlinearity. A phase plot (Fig. 7), where the sample size is plotted against the order parameter clearly shows the nonlinear hysteresis cycle.

Figure 8 shows the layer after five cycles. It is seen that indeed some of the bilayer structure is conserved upon repetitive compression and expansion of the sample. Also the bottom layer (not shown) contains some bilayer structure. The relaxation time of such structures apparently exceeds that of the oscillation period.

### D. Temperature dependence

A similar analysis as was performed above at a temperature of $k_BT = 0.5$ was repeated on a sample at a somewhat lower temperature, at $k_BT = 0.45$. We only present here the results for the order parameter (Fig. 9.). Now there is a slight increase of the order parameter at the initial compression, but it does not return to that high value after the first cycle. Again the order parameter drops steeply when the layer is compressed beyond the maximal lateral density and increases more gradually during the expansion but the behavior is not completely periodic. In the repeated cycles the maximally obtained value decreases, indicative for the increased formation of micellar structures at the interface. The minimal value does not change after the first cycle, and is larger than for the higher temperature. On the other hand, the maximum is smaller, and on average the value of the order parameter is the same, only the amplitude of the fluctuation is smaller. The lower temperature sample exhibits a longer transient than the higher temperature one, and also reacts less to the periodic forcing.

### E. Frequency dependence

Next, we lower the frequency, keeping the sample temperature at $k_BT = 0.5$. When the oscillation period is extended to 200 ns, a 5-MHz oscillation frequency, comparable with what is used in real experiments and applications of oscillating bubbles, the behavior is quite different. We only show the results for the order parameter (Fig. 10). Upon compression

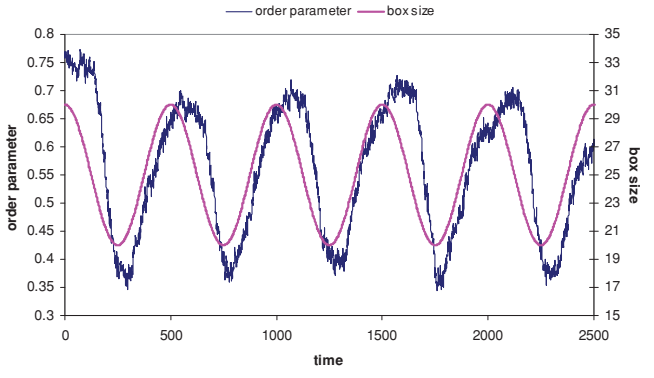


FIG. 6. (Color online) Order parameter (left axis) and box size (right axis) as a function of time (reduced units; one unit is 10 ps). After the first cycle the order parameter does not relax to its original equilibrium value. Inspection of the snapshots shows that some micellar structures remain. The reaction of the order parameter to the imposed box size shows both a phase delay and nonlinearity; the drop upon compression is much faster than the gain upon expansion.

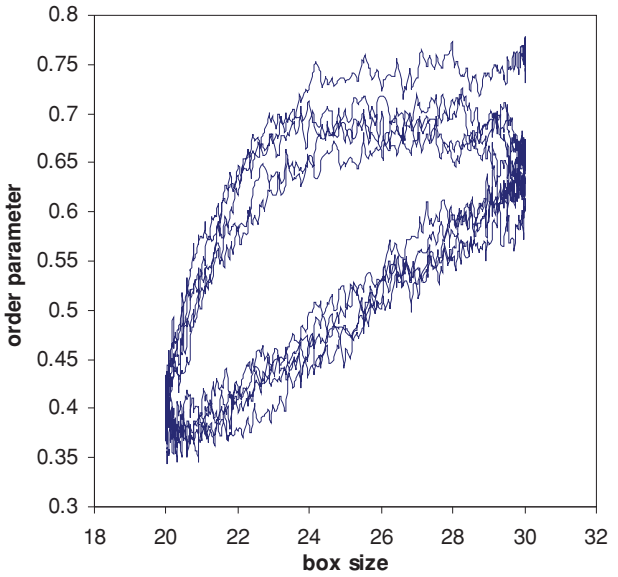


FIG. 7. (Color online) Phase plot of the order parameter as a function of lateral box size for five periods of a 200-MHz sinusoidal oscillation. Motion is counterclockwise. Apart from a phase delay there is also a distinct difference in the upward and downward stroke response. Monolayer order is destroyed more rapidly than it is regained.

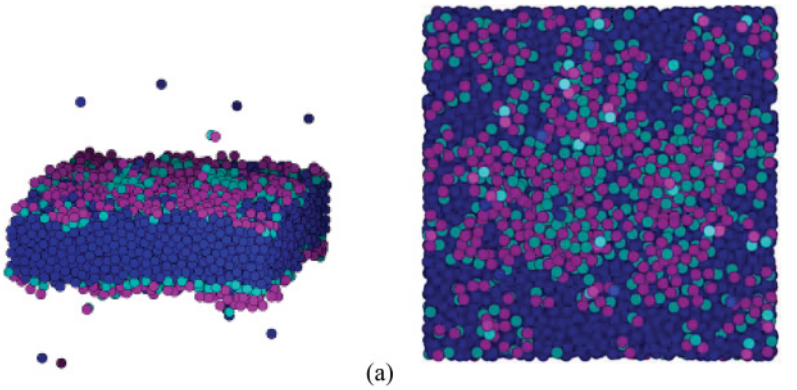


FIG. 8. (Color online) Sample conformation at the end of the five cycles of 5 ns each, at maximal expansion. The sample does not return to a monolayer coating; more complex structures survive the treatment.

from lateral box size 30–25, no effect is seen on the order parameter, quite similar to the high frequency case. When the box size drops below 25 units, lipids become squeezed, and move out of the layer and start forming double layer structures, like at 200 MHz. The minimal value of the order parameter now, however, is reached at maximal compression; there is no clear phase delay. Neither is there any clear sign of nonlinearity in expanding again. At a box size of 25 units the lipids return to the monolayer conformation that breaks into patches upon further expansion.

## IV. DISCUSSION

We have shown that the present coarse grained model allows long simulation runs, on a simple PC, also at low frequencies, due to its relatively simple representation of the constituting molecules. Our simulations show that a compressed monolayer of lipids does fold and form micellelike structures. For high frequency cycles these structures survive upon consequent expansions. If repeated cyclically the micellar structure tends to grow, and the coating layer gradually loses its monolayer character. At higher temperatures this occurs more rapidly, after just one or two cycles. The micellar elements in the coating layer that survive the compression cycle reappear at roughly the same position and in the same orientation, but there is some random drift involved.

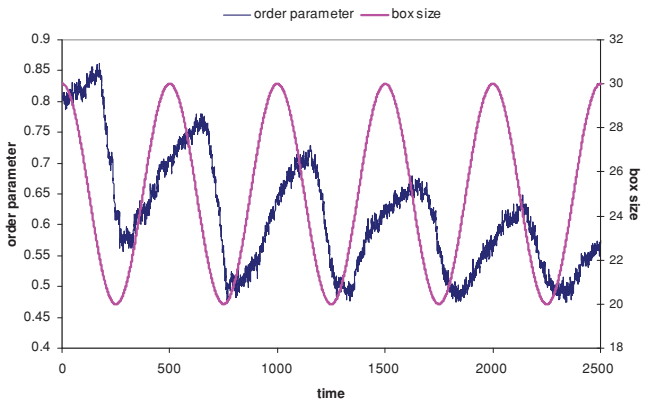


FIG. 9. (Color online) Order parameter (left axis) and box size (right axis) as a function of time (reduced units; one unit is 10 ps) at an ambient reduced temperature of $T = 0.45$. The difference with the higher temperature sample is that the development is spread over several cycles. There also is a small increase at the first compression.

At lower frequencies, comparable to those applied in real experiments and applications, the micellar structures also form upon compression, but largely disappear upon consecutive expansion.

At the lower temperature the water phase of the system has a tendency to crystallize. When it does, expansion leads to rupture of the layer, and formation of a hole (Fig. 11). The assumption of independency of the two layers in such a case obviously cannot be maintained. This phenomenon did only occur in runs at the lower temperature. Still we have several examples of simulation runs at that temperature and oscillation frequencies ranging from 200 to 2 MHz, that do not show freezing of the water phase and subsequent rupture, while similar runs with just a different random seed for the initial thermal velocity distribution do. We performed various series of simulations at the higher temperature, and did not find the freezing to occur in any of the runs as performed.

The dimer lipid model was designed to simulate emulsion stabilization, and the model lipids do indeed reduce the surface tension at an oil-water interface by one to two decades. We have done tests at the vacuum-water interface and found a reduction of 25% in the most expanded samples (box size

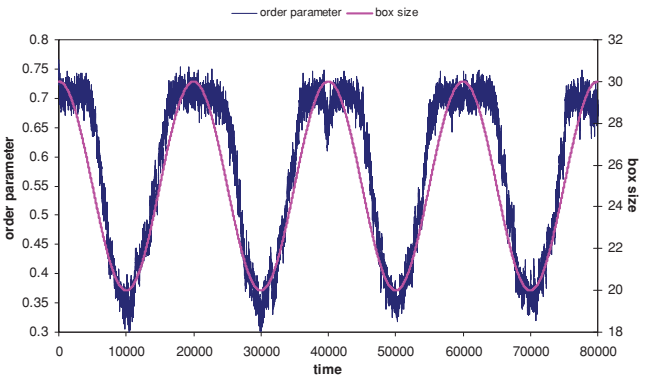


FIG. 10. (Color online) Order parameter (left axis) and box size (right axis) as a function of time (reduced units, one unit is 10 ps) at an ambient reduced temperature of $T = 0.5$ and oscillation frequency of 5 MHz. Between box size 30 and about 25 the sample is in a monolayer conformation that becomes increasingly patchy at higher expansion. Between box size 25 and 20 the sample is compressed to the extent that lipids are squeezed out of the monolayer and form an inverted layer on top of that. The behavior is linear and reversible, without a phase delay.

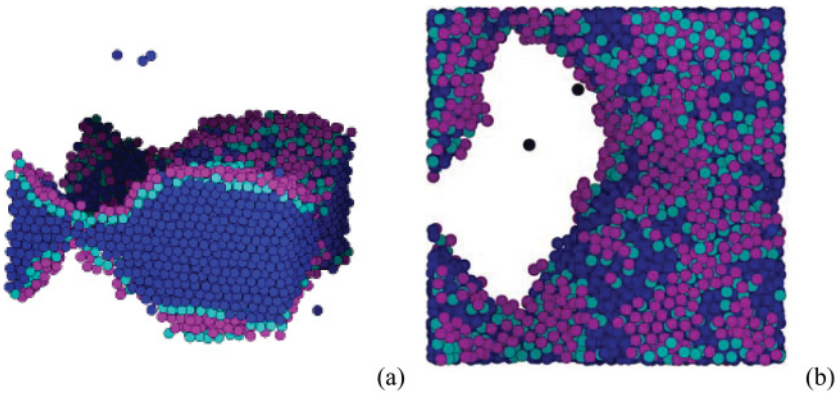


FIG. 11. (Color online) Sample conformation of a low temperature sample at the end of a single cycle of 50 ns, at maximal expansion. The water phase shows a regular crystalline ordering, and it ruptures upon expansion, allowing the two coating layers on opposite sides to come into contact. Also the structure inside the monolayer is increased, with hexagonal patches, and bilayer structures do survive the cycle. Though interesting on its own accord, this sample does not present a valid simulation of the system we set out to model.

30), where about 60% of the surface is covered, to 50% reduction at full coverage (box size 25). The dimers act as a mild surfactant for reducing the surface tension. That does not imply that they do not show a preference for the surface, and also the lateral pressure, responsible for the folding of the coating layer, is shown to behave as expected. In our sample we did not observe macroscopic folding of the monolayer, as has been observed in real monolayers under slow lateral compression [4]. Moreover, the lipids in our simulation move towards the air phase (vacuum) when they are squeezed out of the monolayer, while other simulations suggest that the layer as a whole folds towards the water phase. This probably is caused by the fact that in our model individual lipids can escape the monolayer relatively easily. The structural integrity of the monolayer is not large enough to prevent such events, and hence there is little need for further folding to relax the lateral pressure.

In the simulation we have forcibly changed the size of the sample, as if we change the radius of the bubble. In practice it is the pressure that is influenced by the ultrasound field, and the reaction of the bubble on that modulated field depends on the size of the bubble and the amount of lipid coating present. For small bubbles, the bubble's size oscillates likes the ultrasound field, for larger bubbles at high coating density the bubble size decreases upon compression, but the bubble does not expand beyond its equilibrium size at low pressure [13]. This compression-only behavior is thought to be related to the rupture of the monolayer upon expansion of the bubble, exposing the air-water surface. The high surface tension of the exposed water surface greatly reduces the size of that expansion, while the low surface tension of the coated surface and the ease at which its folds makes it react much more strongly to the compression phase. In our present model the effect of the surface tension of the water is not taken into account sufficiently. The LJ potential is rather weak and the surface tension of a LJ fluid is much smaller than that of the water, where the much stronger electric dipole interaction induces a very large surface tension. As mentioned above, for our model the surface tension of the water phase is not reduced as significantly as it is for real lipid layers on real water.

The behavior of our model system can explain several of the features that occur in real systems, but apparently at a much shorter time than in reality. This may be due to the interaction used between the water particles and the head groups. Micellar structures are coupled much more loosely than in reality, and hence will fall apart much more quickly. The time scale we used is a kinetic one, related to the thermal motion of the quasiparticles in our model compared to those in a real sample, while the dynamic time scale of the multiparticle structures is largely determined by the interactions. The same is valid for the water phase; the effect of hydrogen bridging is poorly described by the LJ potential we used in our model. Possibly a model with a loosely bonded network of particles, similar to the bonded interactions for the dumbbells but only temporarily, can capture those aspects. In extrapolating the observations in this work, one may expect that micellar structures will form at any oscillating surface, even if the lipid concentration in the fluid is well below the critical micelle concentration. For the formation of lipid micelles, which are believed to have played a significant role in the early stages of the chemical history of the earth, hence rather low concentrations can have sufficed, if they occur in conditions where there is an air-water surface that is vigorously and rapidly disturbed.

## ACKNOWLEDGMENT

J.H.J.v.O. wishes to acknowledge the hospitality of the Physics of Fluids of the University of Twente, where he learned about the experiments on coated bubbles during a sabbatical leave.

[1] S. Qin, C. F. Caskey, and K. W. Ferrara, Phys. Med. Biol. **54**, R27 (2009).

[2] S. M. van der Meer, B. Dollet, M. Voormolen, C. T. Chin, A. Bouakaz, N. de Jong, M. Versluis, and D. Lohse, J. Acoust. Soc. Am. **121**, 648 (2007).

[3] G. Pu, M. A. Borden, and M. L. Longo, Langmuir **22**, 2993 (2006).

[4] L. Pocivavsek, S. L. Frey, K. Krishan, K. Gavrilov, P. Ruchala, A. J. Waring, F. J. Walther, M. Dennin, T. A. Witten, and K. Y. C. Lee, Soft Matter **4**, 2019 (2008).

[5] A. Gopal, V. A. Belyi, H. Diamant, T. A. Witten, and K. Y. C. Lee, Phys. Chem. B Lett. **110,** 10220 (2006).
[6] B. Dollet, S. M. van der Meer, V. Garbin, N. de Jong, D. Lohse, and M. Versluis, Ultrasound Med. Biol. **34**, 1465 (2008).
[7] M. Emmer, H. J. Vos, D. E. Goertz, A. van Wamel, M. Versluis, and N. de Jong, Ultrasound in Medicine and Biology **35**, 102 (2009).
[8] A. A. Doinikov, J. F. Haac, and P. A. Dayton, Ultrasonics **49**, 269 (2009).
[9] P. Marmottant, S. M. van der Meer, M. Emmer, M. Versluis, N. de Jong, S. Hilgenfeldt, and D. Lohse, J. Acoust. Soc. Am. **118**, 3499 (2005).
[10] S. Baoukina, L. Monticelli, H. J. Risselada, S. J. Marrink, and D. P. Tieleman, Proc. Natl. Acad. Soc. USA **105**, 10803 (2008).
[11] A. Gopal and K. Y. C. Lee, J. Phys. Chem. B **105**, 10348 (2001).
[12] T. T. Nguyen, A. Gopal, K. Y. C. Lee, and T. A. Witten, Phys. Rev. E **72**, 051930 (2005).
[13] N. de Jong, M. Emmer, C. T. Chin, A. Bouakaz, F. Mastik, D. Lohse, and M. Versluis, Ultrasound in Medicine and Biology **33**, 653 (2007).